Impregnation of γ-Alumina with Ni(II) or Co(II) Ions at Neutral pH: Hydrotalcite-Type Coprecipitate Formation and Characterization

Jean-Baptiste d'Espinose de la Caillerie,† Maggy Kermarec,‡ and Olivier Clause*

Contribution from the Kinetics and Catalysis Division, Institut Français du Pétrole, BP 311, 92506 Rueil-Malmaison Cedex, France, and Laboratoire de Réactivité de Surface, URA 1106 CNRS, UPMC, 4 place Jussieu, 75252 Paris Cedex 05, France

Received November 28, 1994. Revised Manuscript Received August 3, 1995®

Abstract: The adsorption of Co(II) or Ni(II) ammine complexes from aqueous solutions onto γ-alumina at neutral or near neutral pH ($7 < pH < 8.2$) and ambient temperature is investigated as a function of the ion concentration in the impregnating solutions, the contact and aging times, and the drying conditions. The formation of coprecipitates including Al(III) ions extracted from the support is demonstrated by EXAFS and IR spectroscopy for contact times and Ni or Co loadings higher than 0.5 h and about 2.0 wt %, respectively. The EXAFS technique makes it possible to distinguish the Ni or Co hydroxides and basic nitrates from coprecipitates with the hydrotalcite-type structure. In other words, EXAFS is shown to be sensitive to the presence of aluminum in the coprecipitates. Furthermore, in most cases, the M(II)/Al(III) ratio (M = Ni or Co) in the supported coprecipitates can be estimated. Infrared spectroscopy can also be used as a fingerprint of coprecipitate formation through lattice octahedral modes characteristic of the NiAl and CoAl hydrotalcite-type compounds in the 400−450 cm^{-1} region. Thus, alumina should not be considered systematically as inert even at pH values close to its isoelectric point. Possible mechanisms responsible for the formation of coprecipitates at pH values nonaggressive for alumina are discussed. Dialysis experiments leading to the observation of hydrotalcite crystallites at a distance from alumina suggest that a dissolution−precipitation mechanism is possibly involved and that the rate of alumina dissolution is promoted by adsorbed Ni(II) or Co(II) ions. Three phenomena are suggested to occur at the same time at the oxide/water interface; the adsorption of ions, as described by the site binding models; the alumina dissolution, promoted by the adsorbed ions and kinetically limited; the coprecipitation of M(II) with Al(III) ions extracted from the support. Site binding models have a considerable value for the early stages of impregnation, whereas approaches which use geochemistry as a basis and involve surface rehydration and coprecipitate formation have probably a greater validity for the later stages.

Introduction

Metal ion deposition and chemisorption onto oxide surfaces control numerous aspects of colloid chemistry and catalyst manufacture, especially preparation. Ion adsorption phenomena on hydrous oxides are essential to various subfields of geochemistry such as weathering (water/rock interaction), environmental science, water treatment, and precipitate or colloid flotation techniques.[1] Oxide hydrosol stability can be affected by adsorbed ions leading to modifications of the kinetics of coagulation.[2,3] The dissolution of many slightly soluble minerals has often been reported to be a surface-controlled process, which can be promoted or hindered by ligands such as fluoride ions.[4−6] The first step of oxide supported catalyst preparation usually involves the impregnation of the carrier with aqueous solutions containing salts of the metals to be deposited.[7] Ion/support interaction during impregnation or drying plays an important role on the properties of the final catalyst, such as reducibility, resistance against thermal sintering of the active phase, or metal particle dispersion.[8]

When oxide particles are put in contact with aqueous solutions, they usually acquire a charge due to the dissociation of surface hydroxyl groups which may behave for some of them as Brønsted acids and for others as Brønsted bases.[9−11] This observation has led to descriptions of oxide surfaces in terms of distributions of adsorption sites with different strengths, for which many electrical double layer and adsorption models have been proposed in the fields of catalysts,[12] electrochemistry,[13] and colloid science.[14] Physical, electrostatic-type ion/support

* To whom correspondence should be addressed at the Institut Français du Pétrole.

† Present address: Laboratoire de Physique Quantique, URA 1428 CNRS, ESPCI, 10 rue Vauquelin, 75231 Paris Cedex 05, France.

‡ Laboratoire de Réactivité de Surface.

® Abstract published in *Advance ACS Abstracts*, November 1, 1995.

(1) On the selective precipitate flotation of metals, see the review of: Lemlich, R. *Ind. Eng. Chem.* **1968**, *60* (10), 16−29. See also: Crawford, R. J.; Harding, I. H.; Mainwaring, D. E. *Langmuir* **1993**, *9*, 3050−3056 and 3057−3062.

(2) Dumont, F.; Watillon, A. *Discuss. Faraday Soc.* **1971**, *52*, 352−360.

(3) Breeuswa, A.; Lyklema, J. *Discuss. Faraday Soc.* **1971**, *52*, 324−333.

(4) Furrer, G.; Stumm, W. *Geochim. Cosmochim. Acta* **1986**, *50*, 1847−1860.

(5) Wieland, E.; Wehrli, B.; Stumm, W. *Geochim. Cosmochim. Acta* **1988**, *52*, 1969−1981.

(6) Casey, W. H.; Banfield, J. F.; Westrich, H. R.; McLaughlin, L. *Chem. Geol.* **1993**, *105*, 1−15.

(7) Che, M.; Bennett, C. O. *Adv. Catal.* **1989**, *36*, 55−172.

(8) On the role of the ion/support interactions on reducibility and dispersion of metal catalysts, see for example: Louis, C.; Cheng, Z. X.; Che, M. *J. Phys. Chem.* **1993**, *97*, 5703−5712. On the role of preparation on the structure of supported oxide catalysts, see: Williams, C. C.; Ekerdt, J. G.; Jehng, J-M.; Hardcastle, F. D.; Wachs, I. E. *J. Phys. Chem.* **1991**, *95*, 8791−8797.

(9) Parks, G. A.; de Bruyn, P. L. *J. Phys. Chem.* **1962**, *66*, 967−972.

(10) Healy, T. W.; White, L. R. *Adv. Colloid Interface Sci.* **1978**, *9*, 303−345.

(11) Adamson, A. W. *Physical Chemistry of Surfaces*; Wiley: New York, 1982; pp 193−195.

(12) Brunelle, J. P. *Pure Appl. Chem.* **1978**, *50*, 1211−1229.

(13) Yates, D. E.; Levine, S.; Healy, T. W. *J. Chem. Soc., Faraday Trans. 1* **1974**, *70*, 1807−1818.

0002-7863/95/1517-11471$09.00/0

interactions,[12,15,16] coordinative ion/surface bonding,[17-20] lateral interactions between adsorbing ions, and site heterogeneity at oxide surfaces have been invoked.[21-23]

A need for some adjustments of the site-binding models to porous, high surface area oxides was, however, perceptible in numerous studies in the literature. The two-dimensional character of the oxide/electrolyte interface was questioned and counter charge behind the oxide particle surface was considered, by analogy with the diffuse double layers encountered in emulsions.[3,24] The surface charge was thought to be distributed within some depth of a surface layer, which was suggested to be permeable to adsorbing ions. On the other hand, diffusion transfer of ions across a layer of a few tens of angstroms at the surface of minerals was also frequently suggested to be rate-limiting for the dissolution of these minerals.[25-27] Thus, the question arises as to whether the well-documented dissolution precipitation or reconstruction concepts developed to account for natural or artificial weathering processes are also valid during catalyst preparation or ion adsorption on colloids. This idea relies on recent results obtained when Ni(II), Co(II), or Zn(II) ions are deposited onto alumina or silica at neutral pH and ambient temperature: surface coprecipitates including silicon or aluminum ions form directly during impregnation at the oxide/liquid interface.[28,29] Consequently, in aqueous solutions at neutral pH, neither alumina nor silica can be considered systematically as inert suspensions. Furthermore, coprecipitate formation during impregnation has most probably a crucial importance on the characteristics of the calcined or reduced systems, such as the thermal stability of the promoted oxides.[30]

Further investigations of the reactivity of alumina at the oxide/water interface in the presence of metal ions are in order. We performed alumina impregnations through a dialysis membrane and we observed the formation of hydrotalcite-type, aluminum-containing coprecipitates at a distance from alumina. Then, we focused on the alumina/water interface during impregnation. Suitable characterization procedures were chosen in order to distinguish Al-containing coprecipitates from the hydroxides and basic salts which may precipitate onto the oxide surface. In this paper the EXAFS technique and infrared spectroscopy are shown to be well adapted to the determination of the species formed on alumina during impregnation, whereas the XANES spectroscopy confirms that the deposited ions are octahedrally coordinated in the 2+ oxidation state. The alumina impregnation can be seen as an artificial weathering and, as a result, the formation of coprecipitates is reminiscent of the formation of secondary phases during natural weathering.

Experimental Section

Sample Preparation. The samples were prepared by putting in contact 5 g of a commercial γ-Al_2O_3 in powder form (specific surface area, 195 m^2/g; mean pore diameter, 6 nm; pore volume, 0.640 cc/g; major impurities, 1795 ppm TiO_2; 140 ppm Fe_2O_3; isoelectric point: 7.3; traces of α Al_2O_3 visible by XRD, calcination at 700 K during 2 hr before impregnation) with 200 mL of cobalt(II) or nickel(II) nitrate solutions with metal concentrations ranging from 0.01 to 0.1 M containing also 1 M ammonium nitrate. The pH was adjusted to the desired value by bubbling gaseous ammonia. The suspensions were stirred at 298 K during a fixed time, referred to as contact time. The impregnation experiments were performed in polymethylpentene vessels. The Co(II) solutions and suspensions were kept under Ar in order to prevent the oxidation of Co(II) ions, which is favored by ammonia complexation. After centrifugation and washing with a solution containing 1 M ammonium nitrate at the same pH as the final pH of the impregnating solution, the wet samples were kept in air (or under Ar for the Co(II)-containing samples) during a fixed time, hereafter referred to as the aging time. The samples were then characterized by XAS spectroscopy after quenching at liquid nitrogen temperature. Washing with distilled water and drying in an oven at 373 K for 12 h were performed prior to the infrared measurements. The amounts of adsorbed ions were derived from the concentration differences in the impregnation solutions before and after impregnation.

Preparation of Reference Compounds. The preparation of hydrotalcite-like materials $[Ni_{1-x}Al_x(OH)_2](CO_3)_{x/2}\cdot nH_2O$ ($x = 0.25, 0.28, 0.33$) has been reported previously.[31,32] α-$Ni(OH)_2$ was prepared by precipitation from 1 M $Ni(NO_3)_2$ solution at pH 7.2 with sodium hydroxide and washing with distilled water. β-$Ni(OH)_2$ was obtained by submitting α-$Ni(OH)_2$ to hydrothermal treatment at 473 K for 12 h. The $Ni(NO_3)_2\cdot 2Ni(OH)_2$ basic salt was prepared by precipitation of nickel nitrate at pH 7.2 with sodium hydroxide and drying at 293 K without washing.[33] Pickup of CO_2 during the formation or during storage of the basic nitrate was found to be negligible.

The reference compound $[Co_{0.66}Al_{0.34}(OH)_2](CO_3)_{0.17}\cdot nH_2O$ was prepared by coprecipitation from the nitrate salts at 333 K. The pH was monitored and kept constant at 9.2 during coprecipitation by adding continuously an equimolar solution of $NaHCO_3$ and NaOH. The coprecipitate was washed with distilled water at 333 K until a Na_2O content lower than 0.02% w/w was reached and was then dried overnight in an oven at 373 K. $Co(OH)_2$ hydroxide was precipitated from cobalt(II) nitrate at pH 9.0 and 333 K using NaOH as a precipitating agent. The cobalt nitrate solution was decarbonated and the precipitation was performed under argon atmosphere to avoid any oxidation of Co(II) to Co(III) ions. The precipitate was aged in the mother liquor at 333 K under argon for 48 h and was dried at 373 K without exposure to air. Sample formulae as deduced from elemental and thermogravimetric analysis and X-ray diffraction data are gathered in Table 1 for reference compounds. Very broad lines made the determination of lattice parameters difficult for the α-$Ni(OH)_2$ reference compound. A similar difficulty was encountered in the literature.[34] A value of 0.307 ± 0.002 nm could, however, be estimated for the cell parameter a of α-$Ni(OH)_2$.

XAS Measurements. XAS measurements at the Ni and Co K edge were performed at the LURE radiation synchrotron facility (Orsay, France) using the D44 X-ray beamline emitted by the DCI storage ring (positron energy 1.85 GeV; ring current 300 mA). The spectra were recorded at liquid nitrogen temperature in the transmission mode using two air filled ionization chambers. A channel-cut single crystal of silicon was used as the monochromator, the (331) reflection being used.

(14) Davis, J. A.; James, R. O.; Leckie, J. O. *J. Colloid Interface Sci.* **1978**, *63*, 480-499.
(15) Westall, J.; Hohl, H. *Adv. Colloid Interface Sci.* **1980**, *12*, 265-294.
(16) Sprycha, R. *J. Colloid Interface Sci.* **1984**, *102*, 173-185.
(17) Davis, J. A.; Leckie, J. O. *J. Colloid Interface Sci.* **1978**, *67*, 90-107.
(18) Summers, J. C.; Ausen, S. A. *J. Catal.* **1978**, *52*, 445-452.
(19) Hayes, K. F.; Leckie, J. O. *J. Colloid Interface Sci.* **1987**, *115*, 564-572.
(20) Misak, N. R. *Adv. Colloid Interface Sci.* **1994**, *51*, 29-135.
(21) Contescu, C.; Jagiello, J.; Schwartz, J. A. *Langmuir* **1993**, *9*, 1754-1765.
(22) Spanos, N.; Vordonis, L.; Kordulis, Ch.; Lycourghiotis, A. *J. Catal.* **1990**, *124*, 301-314.
(23) Vordonis, L.; Spanos, N.; Koutsoukos, P. G.; Lycourghiotis, A. *Langmuir* **1992**, *8*, 1736-1743.
(24) Lyklema, J. *J. Electroanal. Chem.* **1968**, *18*, 341-348.
(25) Wollast, R. *Geochim. Cosmochim. Acta* **1967**, *31*, 635-648.
(26) Paces, T. *Geochim. Cosmochim. Acta* **1973**, *37*, 2641-2663.
(27) Chou, L.; Wollast, R. *Geochim. Cosmochim. Acta* **1984**, *48*, 2205-2217.
(28) Clause, O.; Kermarec, M.; Bonneviot, L.; Villain, F.; Che, M. *J. Am. Chem. Soc.* **1992**, *114*, 4709-4717.
(29) Paulhiac, J. C.; Clause, O. *J. Am. Chem. Soc.* **1993**, *115*, 11602-11603.
(30) Rebours, B.; d'Espinose de la Caillerie, J. B.; Clause, O. *J. Am. Chem. Soc.* **1994**, *116*, 1707-1717.
(31) Clause, O.; Rebours, B.; Merlen, E.; Trifiro', F.; Vaccari, A. *J. Catal.* **1992**, *133*, 231-246.
(32) Clause, O.; Gazzano, M.; Trifiro', F.; Vaccari, A.; Zatorski, L. *Appl. Catal.* **1991**, *73* 217-236.
(33) Singley, W. J.; Carriel, J. T. *J. Am. Chem. Soc.* **1953**, *75*, 778-781.
(34) Pandya, K. I.; O'Grady, W. E.; Corrigan, D. A.; McBreen, J.; Hoffman, R. W. *J. Phys. Chem.* **1990**, *94*, 21-26.

Table 1. Chemical Composition and X-ray Diffraction Data for Reference Samples[a]

sample	chemical analysis: Ni (wt %)	Co (wt %)	Al (wt %)	M(II)/Al(III) molar ratio	sample formulae	hydroxide or hydrotalcite-like structure lattice constants (nm): *a*	*c*
β-Ni(OH)$_2$	62.0	–	–	–	Ni(OH)$_2$	0.3126	0.4605
Ni basic nitrate	31.4	–	–	–	Ni(NO$_3$)$_2$·2Ni(OH)$_2$·4H$_2$O	0.3050	2.100
NiAl2	37.7	–	8.4	2.0	[Ni$_{0.67}$Al$_{0.33}$(OH)$_2$](CO$_3$)$_{0.16}$·0.45H$_2$O	0.3027	2.272
NiAl2.5	39.7	–	7.4	2.5	[Ni$_{0.72}$Al$_{0.28}$(OH)$_2$](CO$_3$)$_{0.14}$·0.54H$_2$O	0.3035	2.293
NiAl3	40.7	–	6.3	3.0	[Ni$_{0.75}$Al$_{0.25}$(OH)$_2$](CO$_3$)$_{0.12}$·0.50H$_2$O	0.3041	2.317
β-Co(OH)$_2$	–	60.5	–	–	Co(OH)$_2$	0.3183	0.4652
CoAl2	–	38.2	9.3	1.9	[Co$_{0.66}$Al$_{0.34}$(OH)$_2$](CO$_3$)$_{0.17}$·0.61H$_2$O	0.3067	2.268

[a] Note: – indicates that the corresponding element is not present in the sample. The inaccuracy on the lattice parameter values is 5×10^{-4} nm for *a* and 2×10^{-3} nm for *c*.

Our EXAFS station was not equipped with a double mirror harmonic rejection system. However, the harmonic content at three times the energy of the fundamental, i.e., in the 21000–24000 eV range, was low due to the value of the critical wavelength (λ_c = 3.37 Å) and its detection was minimized since the ionization chambers were filled with air. We tested the harmonic contribution to the signal by putting Zr and Ar films (K edges at 17 998 and 25 514 eV, respectively) into the beam and sweeping the energy around 8000–9000 eV. No edge was observed. Thus, the contribution of harmonics could be neglected. The energies were scanned with 2-eV steps for EXAFS analysis. The resolution $\delta E/E$ at the Ni and Co K edges was 2×10^{-4}. EXAFS measurements were carried out three times for each sample. The dried samples were finely ground and homogeneously dispersed in cellulose pellets. The amounts of nickel or cobalt in the pellets were calculated so that the absorption variations $\Delta(\mu x)$ through the edge ranged between 0.8 and 1.2. The wet samples were inserted between two kapton windows then cooled to liquid nitrogen temperature and evacuated before performing EXAFS measurements. The energies were scanned with 0.2-eV steps for XANES analysis except for the preedge regions, which were scanned with 0.1-eV steps. The energies were internally calibrated using a Co or Ni metal foil reference and a third ionization chamber in series with the sample. Data analysis was performed using the University of Washington XAFS analysis package. The χ function was extracted from the data using a Victoreen preedge background and a spline postedge background and normalizing the edge to unity. The same procedure was used to normalize the near-edge structure (XANES), after energy correction using the internal standard. The χ function was Fourier transformed after multiplication by a k or a k^3 factor. The windows are specified in the text. Ab initio amplitude and phase functions were calculated using the FEFF5 codes and tables.[35,36]

IR Spectroscopy. The dried samples were finely ground and dispersed in KBr pellets with a ratio of about 1 mg/100 mg of KBr. The IR spectra were scanned at room temperature using a Bruker FTIR IFS 66V spectrophotometer equipped with a DTGS detector. The spectral conditions consisted of a resolution of 4 cm^{-1}, an aperture of 12 mm, and 30 scans.

X-ray Diffraction Measurements. X-ray powder diffraction analysis was carried out with a Philips PW1820 diffractometer using a copper target and a secondary beam monochromator. The lattice constants were determined by least-squares measurements.

Ni(II) or Co(II) Ion Deposition through a Dialysis Membrane. Alumina in the form of 3 mm diameter spheres was put in contact with distilled water for 3 h so as to fill up the pores. Wet alumina (200 g) was put in a membrane tube (Spectra/por Membrane; MWCO: 6000–8000) which was then sealed. The alumina-containing membrane was immersed in a polymethylpentene flask filled with 2000 mL of a 0.01 M NH_4NO_3 solution at pH 9 whose temperature was thermostatically controlled at 333 ± 2 K. The solution was gently stirred with a magnetic stirrer. A M(II) (M(II) = Ni(II) or Co(II)) solution (0.01 M M(II); 1 M NH_4NO_3) at pH 9 was added dropwise to the ammonium nitrate solution outside the membrane. The rate of M(II) introduction was set at 1 mL/h. The experiment was conducted for 2 weeks under argon atmosphere. The membrane was then removed and the solution filtered. The precipitate was analyzed by X-ray diffraction and the aluminum and nickel (or cobalt) contents determined by atomic absorption after dissolution in nitric acid. The amount of nickel (or cobalt) and aluminum in the solutions after filtration was determined by atomic absorption. Blanks were checked by means of runs conducted at the same conditions of pH and temperature without addition of M(II). For all the determinations of Ni, Co, and Al concentrations in solution, the solutions were acidified with nitric acid before the temperature was lower to ambient and the solutions were then stored in polymethylpentene flasks.

Results

Structure of Reference Compounds. Let us review briefly the structure of the hydroxide and of the hydrotalcite-like phases. β-Ni(OH)$_2$ has the C$_6$-type layered structure with a hexagonal unit cell of dimensions a = 0.3126 nm and c = 0.4605 nm.[37,38] This structure is built of stacked layers, each layer consisting of NiO6 octahedra sharing edges. Ni hydroxide also exists in a modified form, designated as α-Ni(OH)$_2$, whose structure resembles that of β-Ni(OH)$_2$ except that disordered water layers are present between the (001) planes. A contraction of the Ni–Ni distances in the octahedral layers of approximately 0.005 nm is observed in comparison to β-Ni(OH)$_2$.[34,37] The Ni(NO$_3$)$_2$·nNi(OH)$_2$·mH$_2$O ($2 < n < 8$) basic salts also have the CdI$_2$ structure and are obtained from the α-Ni(OH)$_2$ structure by replacing some OH by NO_3 groups.[39] Reported a and c values range from 0.305 to 0.310 nm and from 0.69 to 0.95 nm, respectively, depending on n. Nickel–aluminum hydrotalcite-type coprecipitates have a structure similar to that of β-Ni(OH)$_2$ except that some Ni(II) are replaced by Al(III) ions in the octahedral layers. This results in positively charged octahedral layers so that the presence of anions, such as carbonate, nitrate, or chloride ions is required for the electrical balance of the structure. The anions are located between the cation-containing shells along with molecules of water hydration. The cations are homogeneously distributed within the octahedral layers.[40]

α and β forms of Co(OH)$_2$ are also known. The cell parameters for the C$_6$ β form are a = 0.3173 nm and c = 0.4640 nm.[41] For α-Co(OH)$_2$ a is reported to be slightly lower (a =

(35) Rehr, J. J.; Mustre de Leon, J.; Zabinski, S. I.; Albers, R. C. *J. Am. Chem. Soc.* **1991**, *113*, 5135–5140.
(36) Mustre de Leon, J.; Rehr, J. J.; Zabinski, S. I.; Albers, R. C. *Phys. Rev. B* **1991**, *44*, 4146–4156.
(37) McEwen, R. S. *J. Phys. Chem.* **1971**, *75*, 1782–1789.
(38) Wells, A. F. *Structural Inorganic Chemistry*; Clarendon Press: Oxford, 1990; pp 631–632.
(39) See: *Gmelins Handbuch der Anorganischen Chemie*; Verlag Chemie: Weinheim, 1966, Vol. 57, pp 524–526. On the structure of basic salts, see also: Wells, A. F. *Structural Inorganic Chemistry*; Clarendon Press: Oxford, 1990; pp 644–645. Hulliger, F. *Structural Chemistry of Layer-type Phases*; Levy, F., Ed.; Reidel Publishing Company: Boston, 1976; pp 279–285.
(40) Cavani, F.; Trifiro', F.; Vaccari, A. *Catal. Today* **1991**, *11*, 173–302.
(41) See: *Gmelins Handbuch der Anorganischen Chemie*; Verlag Chemie: Weinheim, 1961; Vol. 58, pp 498–506.

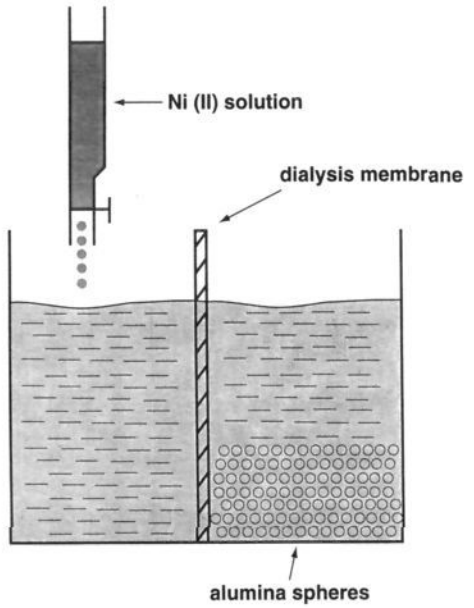

Figure 1. Diagram of the experiment involving a dialysis membrane and leading to the observation of coprecipitates at a distance from alumina. Note that the solution was gently stirred.

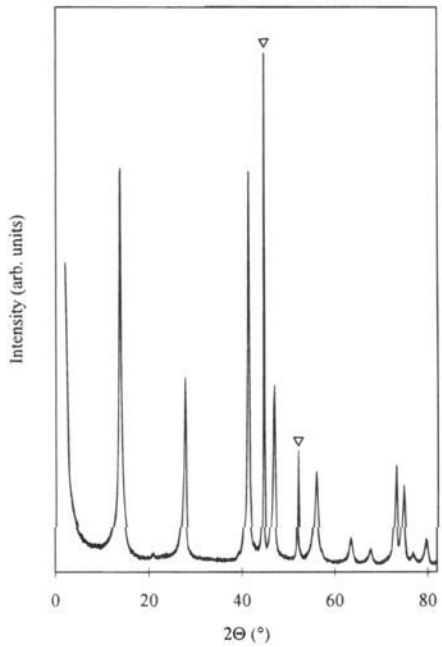

Figure 2. X-ray diffraction pattern of the precipitate obtained outside the bag after filtration and washing (▽ aluminum sample holder).

0.309 nm) than in β-$Co(OH)_2$. The structures of the cobalt− and nickel−aluminum hydrotalcite-like phases are identical.

Growth of Hydrotalcite-Type Compounds at a Distance from Alumina. The principle of this experiment is illustrated in Figure 1 and explained in the Experimental Section. This experiment was inspired by the work of Caillere and Henin on the synthesis of silicates from gels separated by dialysis bags.[42] A 10^{-2} M M(II) (M = Ni or Co) solution at pH 9 was added dropwise outside the dialysis bag containing the alumina spheres. A cloud appeared prpgressively inside *and outside the bag*. After 2 weeks the bag was removed and the solution was filtered. The cloud was, in fact, a precipitate, which was green-blue in the case of Ni(II) addition and pink in the case of Co(II) addition. This precipitate was washed with distilled water, dried in an oven at 373 K for 12 h, and weighed. About 100 mg were obtained.

The composition of the precipitates were determined by flame−atomic absorption spectrometry. In the case of nickel addition, nickel was found (31.5 Ni wt %) as expected but the most interesting result was the presence of aluminum (9.9 Al wt %), corresponding to a Ni/Al atomic ratio of 1.5. The thermogravimetric profile of the coprecipitate was found to be very similar to that of hydrotalcite, exhibiting characteristic H_2O and NO weight losses. Carbonate ions were not detected.

The X-ray diffraction pattern of the coprecipitate revealed a well-crystallized hydrotalcite-like structure, see Figure 2, with cell parameters of $a = 0.3011$ nm and $c = 2.245$ nm. No other crystallized phase was observed. A linear relationship was observed between the cell parameter a of the sample and of the NiAl2, NiAl2.5, and NiAl3 references and the aluminum content. In other words, the lattice parameters of the NiAl hydrotalcite-type compounds obey Vegard's law in the molar ratio range $1.5 < Ni/Al < 3$. This result suggests that no amorphous phase, such as amorphous alumina or nickel hydroxide, was present in addition to the hydrotalcite phase in the filtered coprecipitate. Based on the elemental, XRD, and thermogravimetric analyses, the following formula can be proposed for the precipitate removed after a 2-week Ni addition: $[Ni_{0.60}Al_{0.40}(OH)_2](NO_3)_{0.40}\cdot 1.1H_2O$. This result was found to be very reproducible. Identical coprecipitates were obtained independently of the volume of solution/alumina ratio, ammonium nitrate concentration, and rate of Ni(II) addition, provided the latter was not too high.

Given the weight and the aluminum content of the coprecipitate, the amount of aluminum passed through the membrane can be estimated to be higher or equal to 10 mg. A blank experiment was conducted in order to determine the alumina solubility and the rate of alumina dissolution at 333 K, 10^{-2} M ammonium nitrate, and pH 9 without Ni(II) addition.[1] The aluminum concentration at equilibrium, as measured after acidification at 333 K in a polymethylpentene flask, was attained after 2 weeks and was found to be 0.02 mg/L. Thus, the amount of Al(II) ions which passed the membrane over 2 weeks did not exceed 0.04 mg. By comparing this value to the amount of aluminum in the coprecipitate, namely 10 mg, it was found that the addition of Ni(II) enhanced the rate of alumina dissolution (through the formation of coprecipitates) by a factor of more than three orders of magnitude. Thus, alumina dissolution can be driven by coprecipitate formation with Ni-(II) ions. Very similar results were obtained upon cobalt addition.

Now, a question is, does coprecipitate formation also occur during alumina impregnation with Ni(II) or Co(II) ions at pH 9, or even at neutral pH, i.e., at a pH normally nonaggressive for alumina? Wet and dry Ni/Al_2O_3 and Co/Al_2O_3 samples were prepared at pH 7.2 and 8.1, respectively, and analyzed by X-ray diffraction. Actually, for Ni and Co contents higher than approximately 10 wt %, reflections characteristic of the presence of hydrotalcite-type coprecipitates were detected.[29] However, for lower metal loadings only broad and poorly defined reflections were observed. It could not be specified whether hydroxides, basic salts, coprecipitates, or some other species had been formed in the samples. We performed EXAFS at the Ni and Co K edges to gain more insight into the local environment around the deposited Ni(II) and Co(II) ions.

EXAFS Analysis of the Reference Compounds. α- and β-$Ni(OH)_2$ and $Co(OH)_2$ phases and several nickel−aluminum and cobalt−aluminum hydrotalcite-type coprecipitates were

(42) Besson, H.; Caillere, S.; Hénin, S. *Bull. Groupe Fr. Argiles* **1973**, *26*, 79−89.

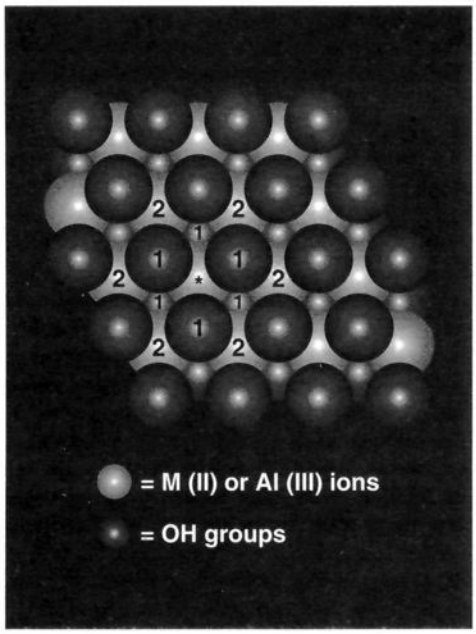

Figure 3. Ball model of an octahedral layer of a hydroxide, basic salt, or hydrotalcite-like compound (top view). A cation is marked with an asterisk, the next nearest cations are marked with a 2. The oxygen ions marked with a 1 belong to the surface and to the underlying oxygen layers.

prepared and used as reference compounds for EXAFS and IR analysis. In previous work, the phase and amplitude functions for the Ni··O, Ni··Ni, and Ni··Al absorber−backscatterer pairs were extracted from the spectra of NiO, β-$Ni(OH)_2$, and a solid solution of Ni^{2+} in β-$Mg(OH)_2$, respectively.[31] While the oxygen nearest coordination shell was correctly described, the distances of the Al next nearest backscatterers and the Ni/Al atomic ratios in the hydrotalcite-type coprecipitates were overestimated. In this work, we performed EXAFS analysis using the theoretical curved wave amplitude and phase functions calculated by the FEFF 5 program of Rehr and co-workers.[35] Before investigating the Ni/Al_2O_3 and Co/Al_2O_3 samples, we tested these functions on hydroxide, basic nitrate, and hydrotalcite-like compounds. We evaluated the reliability of the determination by EXAFS of structural parameters by modifying analysis variables such as the weighing scheme.

An octahedral sheet is shown in Figure 3. Let us specify the composition of the nearest backscatterer shells around the cation marked with an asterisk. The nearest and the next nearest backscatterers are marked with 1 and 2, respectively. The nearest backscatterers are six oxygen atoms belonging to OH groups independently of the presence of aluminum ions in the layers. In the case of hydroxides and basic salts, the next nearest backscatterers are six Ni cations, located at distances ranging from 0.307 to 0.313 nm, whereas in the case of hydrotalcite-type compounds, the next nearest backscatterers are N_{Ni} nickel mixed with N_{Al} aluminum backscatterers located at distances ranging from 0.302 to 0.305 nm with $N_{Ni} + N_{Al} = 6$.[31] Thus, the composition of the next nearest coordination shell makes it possible to distinguish the hydroxide or basic salts from the hydrotalcite-type compounds.

The k^3 weighed EXAFS at the Ni K edge of hydroxide, basic nitrate, and hydrotalcite-type reference compounds are shown in Figure 4. It can be seen that the EXAFS of the α and β hydroxides and of the basic nitrate are very similar. We observe that the basic salt is indistinguishable from α-$Ni(OH)_2$. On the contrary, the EXAFS for hydrotalcite-type compounds can be distinguished from that for hydroxides and basic nitrates, in particular in the 4−6 $Å^{-1}$ range where the Al contribution is significant, or in the 7−9 $Å^{-1}$ range. Thus, the EXAFS technique is sensitive to the presence of aluminum in the octahedral layers.

Fourier transforms were performed using a 2.5−17.5 Å Hanning window after multiplication by a weighing factor of k or k^3. The contributions of O and Ni in the case of hydroxides and of O, Ni, and Al in the case of hydrotalcite references and samples were isolated by inverse Fourier transformation of the data. The range used was $1.2 < R < 3.2$ Å. Curved wave amplitude and phase functions for the Ni··O, Ni··, and Ni··Al absorber−backscatterer pairs were calculated by the FEFF5 program. The fits were done in R-space on both real and imaginary parts of the Fourier transforms. The threshold energy was shifted by a small value ΔE_0, which was minimized during the curve-fitting procedure. Structural parameters obtained from the EXAFS analysis using a k or a k^3 weighing scheme are indicated in Table 2. It can be seen that the number of backscatterers and distances are in good agreement with the XRD data, independently of the weighing scheme. As expected, the Ni−Ni distances are shorter in α-$Ni(OH)_2$ than in β-$Ni(OH)_2$, and the basic nitrate and α-$Ni(OH)_2$ reference compounds are indistinguishable.

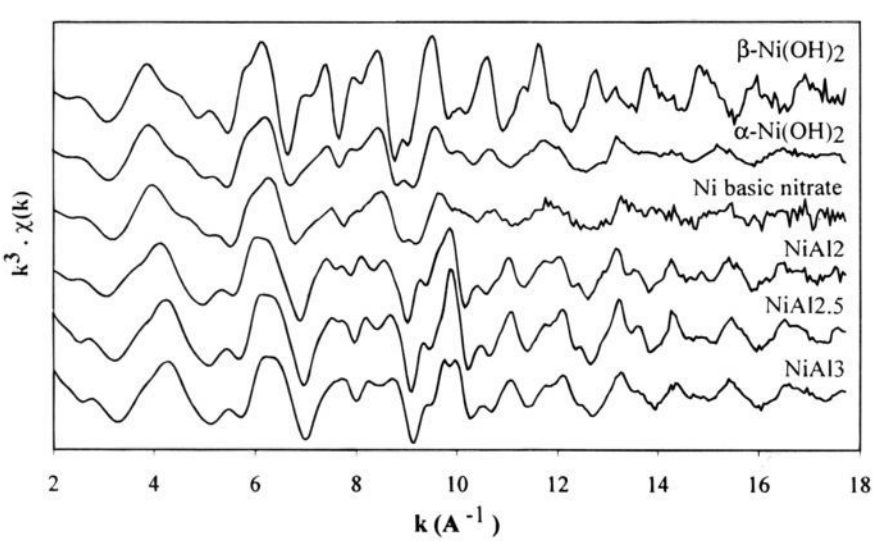

Figure 4. k^3 weighed EXAFS at the Ni K edge of Ni hydroxide, basic nitrate, and Ni−Al hydroxide-like reference compounds.

Table 2. Structural Parameters of Reference Compounds As Determined by EXAFS at the Co and Ni K Edges[a,b]

sample	k^n	backscatterer	N	R (Å)	$10^3\sigma$ (Å)	ΔE_0 (eV)	M(II)/ Al(III)
α-Ni(OH)$_2$	3	O	5.1	2.03	5.5	4.0	
		Ni	5.1	3.08	7.9		−
Ni basic nitrate	3	O	4.8	2.03	5.5	−2.0	
		Ni	5.0	3.09	9.9		−
β-Ni(OH)$_2$	3	O	5.1	2.05	4.0	1.6	
		Ni	5.2	3.12	3.2		−
NiAl2	1	O	5.6	2.05	4.5	3.4	
		Ni	3.7	3.04	4.6		1.6
		Al	2.3	3.04	4.6		
	3	O	5.5	2.04	4.5	1.8	
		Ni	3.4	3.03	4.2		1.7
		Al	2.0	3.03	4.2		
NiAl2.5	3	O	5.4	2.05	4.5	3.5	
		Ni	3.6	3.03	3.9		2.1
		Al	1.7	3.03	3.9		
NiAl3	3	O	6.5	2.05	7.3	−3.1	
		Ni	4.8	3.06	7.8		3.4
		Al	1.4	3.06	7.8		
β-Co(OH)$_2$	3	O	5.3	2.09	5.0	−0.4	
		Co	5.4	3.17	5.8		−
CoAl2	3	O	5.4	2.08	6.2	0.1	
		Co	3.7	3.08	6.9		2.2
		Al	1.7	3.08	6.9		

[a] N, R, σ, and ΔE_0 stand for the coordination numbers, radial distances, Debye−Waller factors, and inner potential corrections, respectively. [b] Estimated precision: N, ±20%, R, ±2%; σ, ±20%; ΔE_0, ±20%; M(II)/Al(III), ±20%.

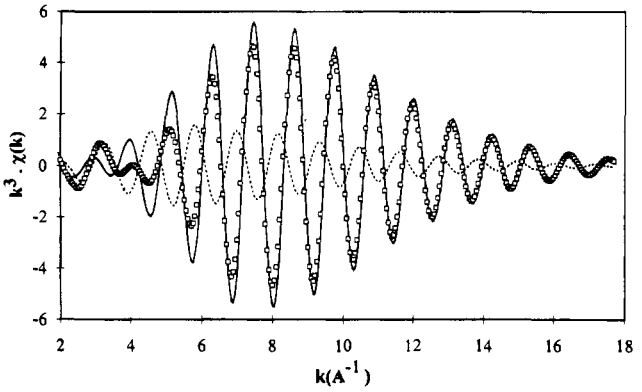

Figure 5. Fourier backtransform of the next nearest backscatterer peak ($2.2 < R < 3.2$) for sample NiAl3 (squares) with the calculated contributions of Ni (solid lines) and Al (dashed lines) backscatterers as determined after fitting procedures. The corresponding structural parameters (best fit) are given in Table 2.

The Ni−Ni and Ni−Al distances were constrained to be equal during the fitting procedures including the aluminum contribution. This constraint was dictated by the hydrotalcite structure. On the other hand, the Debye−Waller factors used for the Ni··Ni and Ni··Al absorber−backscatterer pairs were constrained to remain equal during the fitting procedures. This constraint seems reasonable since Ni and Al backscatterers play similar roles in the octahedral layers and since the thermal disorder, which depends on the backscatterer atomic numbers, was minimized by recording the spectra at the liquid nitrogen temperature. The number of parameters used to fit the data was hence reduced to 8. The statistically justified number was 19, estimated from the Brillouin theorem, $n = 2\Delta k\Delta R/\pi$, where Δk and ΔR are the ranges used for the forward and inverse Fourier transforms (Δk = 15 Å^{-1}, ΔR = 2 Å). We observed that the Ni/Al ratios as determined by EXAFS were close to those determined by elemental analysis independently of the weighing scheme. Also, the Ni−Ni(Al) distances are in good agreement with the XRD results. The inverse Fourier transform of the next nearest backscatterer peak for sample NiAl3 ($2.2 < R < 3.2$ Å range) is shown in Figure 5 along with the contributions of nickel (solid lines) and aluminum (dashed lines) backscatterers as determined by fitting procedures. It can be seen, first, that the contributions of the nickel and aluminum backscatterers, which are located at the same distance, are in phase opposition. This phase opposition leads to the decrease of the height of the next nearest backscatterer peak in the radial distributions as the Al content in the coprecipitates increases, see supporting information. Second, the aluminum contribution is significant at low k values, typically 3−6 Å^{-1}, whereas the nickel contribution is preponderant for higher k values. These features make it possible to distinguish the hydroxides from hydrotalcites by EXAFS, in particular in the 4−6 Å^{-1} k range. A full statistical analysis of the data including the statistical errors in the data points is available as supporting information.

Very similar conclusions were reached at the Co K edge. The k^3 weighed EXAFS at the Co K edge of β-Co(OH)$_2$ and of a cobalt−aluminum hydrotalcite-type coprecipitate with a Co/Al atomic ratio equal to 2.0 are shown in Figure 6. As in the case of Ni, these spectra can be readily distinguished, which is attributable to the presence of aluminum inside the octahedral layers. The analysis of the hydrotalcite-type reference was performed over the 2.5−15.0 Å^{-1} range and Fourier backtransforms were performed over the 1.2−3.2 Å range so as to include the contributions of O, Co, and Al backscatterers without filtering the O shell. We observed that k^3 as well as a k^1 weighing scheme allowed a correct determination of the Co/Al ratio in the coprecipitate. Conclusions similar to those reached at the Ni K edge can be drawn: EXAFS can be used to distinguish aluminum-containing, hydrotalcite-type compounds from hydroxides and basic salts. EXAFS can also be used to estimate the Co/Al ratio in the coprecipitates.

EXAFS Analysis of the Ni/Al$_2$O$_3$ and Co/Al$_2$O$_3$ Samples. Characteristics (metal content, impregnation, aging and drying parameters) of representative samples are gathered in Table 3. The definition of aging time, namely the time between centrifugation and EXAFS analysis after quenching at the liquid nitrogen temperature, is somewhat arbitrary, since some aging may occur during impregnation or washing. Nevertheless, it approximates the time between impregnation and characterization. The influence of the initial Ni(II) concentration was also investigated. k^3 weighed EXAFS of samples prepared in different conditions, wet or dry, are shown in Figure 7 at the Ni K edge and in Figure 6 at the Co K edge. The spectra of the Ni basic salt and of the NiAl2 hydrotalcite-type reference compound are also shown for the record in Figure 7. From a simple examination of Figures 6 and 7 and prior to any mathematical treatment, it appears that the Ni environment in the samples is similar to that of Ni in hydrotalcite-type compounds. This observation is valid for all samples reported in Table 3.

A more detailed analysis of the EXAFS data was performed in order to confirm that NiAl hydrotalcite-type coprecipitates had been formed during the preparation of the samples. The signal is significant up to approximately 15 Å^{-1}, see Figure 7, except for sample Ni4 (3.1 Ni wt %) for which a signal is observed up to 12 Å^{-1} only. Accordingly, the Hanning window used for the Fourier transform was 2.5−15 Å^{-1} (2.5−12 Å^{-1} for sample Ni4). As in the case of the standard compounds, both the real and the imaginary parts of the Fourier transforms were analyzed over the 1.2−3.2 Å range. The structural infor-

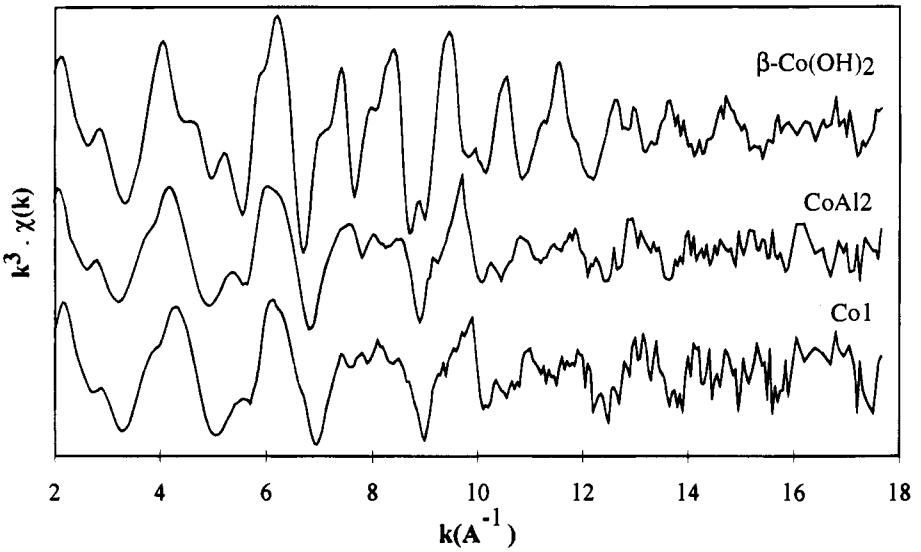

Figure 6. k^3 weighed EXAFS at the Co K edge of the β-$Co(OH)_2$ and $CoAl_2$ references and of the Co1 sample.

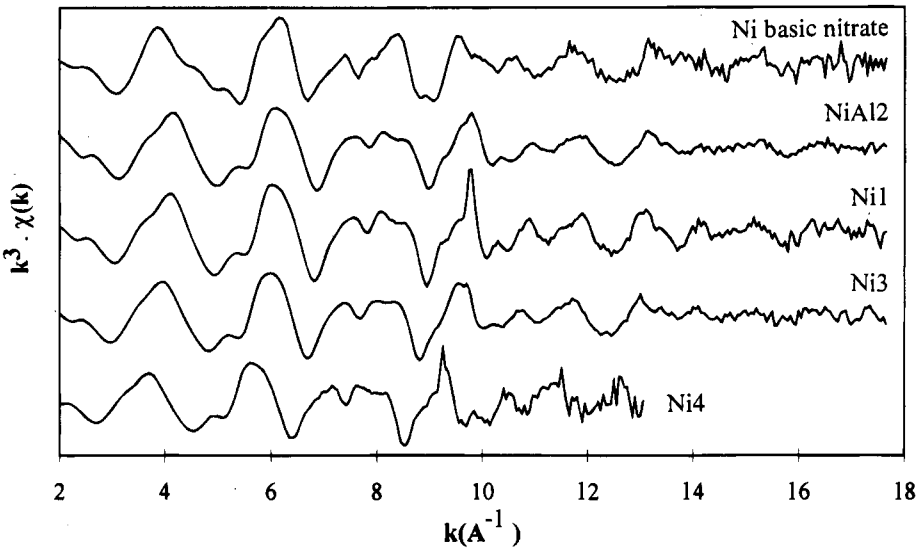

Figure 7. k^3 weighed EXAFS at the Ni K edge of the Ni basic nitrate, the NiAl2 reference before hydrothermal treatment, Ni1, Ni3, and Ni4 samples.

Table 3

sample	Ni or Co wt %	contact time (h)	aging time (h)	wet or dry	initial M(II) concn (M)
Ni1	6.4	1.5	0.25	wet	0.05
Ni2	6.4	1.5	0.25	dry	0.05
Ni3	7.0	1.0	0.25	wet	0.1
Ni4	3.1	0.3	0.25	dry	0.05
Ni5	13	3.5	0.25	wet	0.1
Ni6	13	3.5	8	wet	0.1
Co1	2.4	1.0	0.25	wet	0.01
Co2	2.7	1.0	0.25	wet	0.015

mation extracted from the EXAFS data is gathered in Table 4. Constraints between parameters were identical to those used for the analysis of the references. In all samples, the Ni(II) ions are octahedrally coordinated. The formation of hydrotalcites is confirmed. Since hydrotalcites are observed both in the wet and dry products, the coprecipitation of Ni(II) with Al(III) ions likely occurs during impregnation. The formation of minor amounts of hydroxide or basic salts cannot be excluded: however, since EXAFS averages over all Ni-containing species present in the samples, hydrotalcite is preponderant in all samples.

It can be seen in Table 4 that the Ni/Al atomic ratio in the coprecipitates is dependent on the Ni concentration in the impregnating solution. An increase of the Ni concentration in the impregnating solution results in an increase of the Ni/Al ratio in the hydrotalcite-type coprecipitate (compare samples Ni2 and Ni4 with samples Ni3, Ni5, and Ni6). Conversely, the effect of drying is found to be small (compare samples Ni1 and Ni2). Aging greatly enhances the coprecipitate crystallinity without affecting notably its composition (compare samples Ni5 and Ni6).

The XANES spectroscopy also provides information on the symmetries and oxidation states of the Ni and Co ions in the Ni/Al_2O_3 and Co/Al_2O_3 samples and reference compounds.[43,44] The spectra include two distinct regions: the pre-edge peak (prepeak) corresponds to transitions of 1s electrons to empty levels of partly 3d character and the intense feature centered around the edge is due to dipole allowed 1s → 4p transitions. Increasing the oxidation state shifts the prepeak toward higher energies, whereas the prepeak intensity is related to the Ni(II) symmetry. The prepeak intensity is much higher for Ni(II) or Co(II) in tetrahedral coordination than for Ni(II) or Co(II) in

(43) Pickering, I. J.; George, G. N.; Lewandowski, J. T.; Jacobson, A. J. *J. Am. Chem. Soc.* **1993**, *115*, 4137–4144.

(44) Bianconi, A. *X-ray absorption: Principles, Applications and Techniques of EXAFS, SEXAFS and XANES*; Koningsberger, D. C., Prins, R. Eds.; Wiley: New York, 1988; pp 573–662.

Table 4. Structural Parameters of Samples As Determined by EXAFS at the Co and Ni K Edges[a,b]

sample	k^n	backscatterer	N	R (Å)	$10^3\sigma$ (Å)	ΔE_0 (eV)	M(II)/ M(III)
Ni1	3	O	5.9	2.05	8.1		
		Ni	4.0	3.05	7.0	−1.0	2.2
		Al	1.8	3.05	7.0		
Ni2	3	O	5.6	2.05	7.7		
		Ni	3.6	3.05	7.3	−1.5	1.8
		Al	2.0	3.05	7.3		
Ni3	3	O	5.2	2.05	5.2		
		Ni	3.6	3.05	6.9	−0.5	2.4
		Al	1.5	3.05	6.9		
Ni4	3	O	5.6	2.05	6.3		
		Ni	3.6	3.04	5.3	2.6	1.4
		Al	2.5	3.04	5.3		
Ni5	3	O	5.5	2.05	7.7		
		Ni	4.4	3.07	8.4	1.0	2.9
		Al	1.5	3.07	8.4		
Ni6	3	O	5.3	2.05	9.4		
		Ni	4.2	3.06	7.3	2.0	2.6
		Al	1.6	3.06	7.3		
Co1	3	O	5.1	2.08	5.5		
		Co	3.0	3.09	7.0	4.6	1.4
		Al	2.2	3.09	7.0		
Co2	3	O	5.1	2.08	5.2		
		Co	2.7	3.08	5.7	4.8	1.2
		Al	2.3	3.08	5.7		

[a] N, R, σ, and ΔE_0 stand for the coordination numbers, radial distances, Debye−Waller factors and inner potential corrections. [b] Estimated precision: N, ±20%; R, ±2%, σ, ±20%, ΔE_0, ±20%; M(II)/Al(III), ±20%.

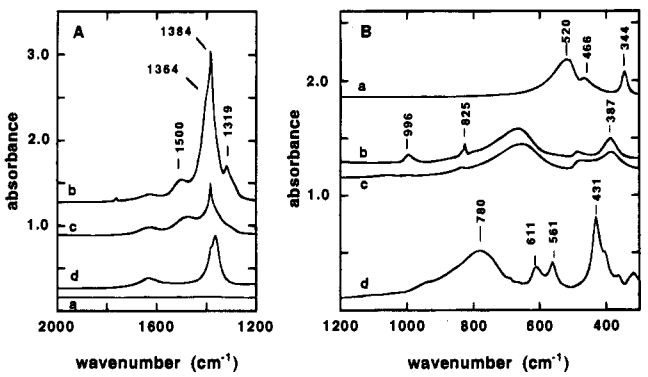

Figure 8. (A) IR spectra in the 2000−1200 cm^{-1} range of (a) β-Ni$(OH)_2$, (b) Ni basic nitrate, (c) α-Ni$(OH)_2$, and (d) NiAl2.5. (B) IR spectra in the 1200−250 cm^{-1} range of (a) β-Ni$(OH)_2$, (b) Ni basic nitrate, (c) α-Ni$(OH)_2$, and (d) NiAl2.5.

octahedral coordination.[43] The near edge structures for the samples and reference compounds are available as supporting information along with the detailed XANES analysis. The XANES analyses at the Ni and Co K edges are consistent with the EXAFS analyses indicating the presence of hydrotalcite in the samples. Also, the XANES spectroscopy provides an independent confirmation that the ions are octahedrally coordinated in the 2+ oxidation state.

Characterization by Infrared Spectroscopy. (a) Characterization of the Reference Compounds. Figure 8A,B displays the spectra of β-Ni$(OH)_2$, $Ni(NO_3)_2{\cdot}2Ni(OH)_2{\cdot}4H_2O$, α-Ni$(OH)_2$, and NiAl2.5 (spectra a−d, respectively). These compounds are characterized by molecular vibrations of structural OH groups bonded to Ni and/or Al atoms, NO_3^- or CO_3^{2-} ions, and lattice vibrations of NiO_6 and/or AlO_6 octahedra.

Let us first examine the information given by the anion vibrations. The nickel hydroxides differ from the other compounds since atoms (nitrate or carbonate) are not included in the structure as for the basic nitrate and the hydrotalcite. However, some nitrate or carbonate ions may remain adsorbed on the α-hydroxide, due to air contamination or insufficient washing. The basic nitrate salt (spectrum b) exhibits bands characteristic of the nitrate (NO_3^-) (1384 and 825 cm^{-1}) and the nitrato ($-ONO_2$) groups (bands at 1500−1319 and 996 cm^{-1}).[45-47] The nitrato groups indicates a covalent character for the Ni nitrate bond. It can be observed that well-crystallized β-Ni$(OH)_2$ contains neither adsorbed nitrate groups nor interlayer H_2O molecules in contrast to the poorly crystallized α-hydroxide (spectra a and c, respectively). NiAl2.5 shows a band with a maximum at 1364 cm^{-1} characteristic or carbonate groups together with a shoulder around 1384 cm^{-1}, showing the presence of residual nitrates which were not detected by thermogravimetry coupled with mass spectrometry. These maxima, corresponding to the most intense vibrations of the carbonate and nitrate groups, are weakly shifted as compared to the values for the free anions (1415 and 1390 cm^{-1}, respectively.[48] This indicates a weak perturbation of electrostatic character in the interlayer space.

Vibrations of structural OH groups and lattice modes can be observed in the 1200−250 cm^{-1} range, see Figure 8B. For Ni hydroxide, the structural OH groups (δ_{OH} and γ_{OH} vibrations) were shown to be very sensitive to the presence of interlayer water molecules.[49] These modes are respectively observed at 520 and 344 cm^{-1} for β-Ni$(OH)_2$, while they are shifted to 654 and 384 cm^{-1} for α-Ni$(OH)_2$. The band around 466 cm^{-1} corresponds to a Ni−O vibration.[50] The spectra of the basic nitrate and the α hydroxide (spectra b and c) are quite similar in the 750−250 cm^{-1} range and correspond to the same vibrations.

The presence of aluminum atoms in the octahedral layers in the hydrotalcite structure gives rise to a modified spectrum. The spectrum of the NiAl2.5 reference compound (Figure 8B, spectrum d) shows, in the 630−250 cm^{-1} range, sharp bands at 431 (the most intense band with a shoulder around 402 cm^{-1}), 611, 561, 364, and 318 cm^{-1}. In the higher frequency range, a broad and asymmetric band at 780 cm^{-1}, with shoulders around 940, 860, 690, and 660 cm^{-1}, is observed. This spectrum is very similar to the spectrum reported by C. J. Serna et al. for a Ni/Al = 2 hydrotalcite (broad bands at 820 cm^{-1} with shoulders at 995, 870, and 690 cm^{-1} and sharp bands at 620, 560, 435 (most intense band), 365, and 335 cm^{-1}).[51] This author assigned bands at 335, 365, 435, 560, and 820 cm^{-1} to translational motions of oxygen in AlO_6 octahedra. The sharpness of the bands is consistent with an ordered distribution of aluminum ions within the octahedral layers. Bands at 620 and 995 cm^{-1} were assigned to OH groups while bands at 870 and 690 cm^{-1} characterized carbonate groups. The position of carbonate groups is well-known whereas bending OH groups bound to Ni or Al atoms may be observed in a higher frequency range. Deuteration experiments were performed in order to strengthen the OH assignments. Deuteration of the NiAl2.5 sample modified only the broad band at 780 cm^{-1}, and indicated the presence of OH groups around 880 cm^{-1}. Therefore, in our sample, the 611 cm^{-1} band seems to belong to a lattice mode.

(45) Addison, C. C.; Gatehouse, B. M. *J. Chem. Soc.* **1960**, 613−616.
(46) Gatehouse, B. M.; Livingstone, S. E.; Nyholm, R. S. *J. Chem. Soc.* **1957**, 4222−4225.
(47) Brand, J. C. D.; Cawthon, T. M. *J. Am. Chem. Soc.* **1955**, *77*, 319−323.
(48) Herzberg, G. *Infrared and Raman Spectra of Polyatomic Molecules*; Van Nostrand: New York, 1945; p 178.
(49) Le Bihan, S.; Figlarz, M. *J. Catal. Growth* **1972**, *13*, 458−461.
(50) Ferraro, J. R. *Low Frequency Vibrations of Inorganic and Coordination Compounds*; Plenum Press: New York, 1971; p 74.
(51) Hernandez-Moreno, M. J.; Ulibari, M. A.; Rendon, J. L.; Serna, C. J. *Phys. Chem. Miner.* **1985**, *12*, 34−38.

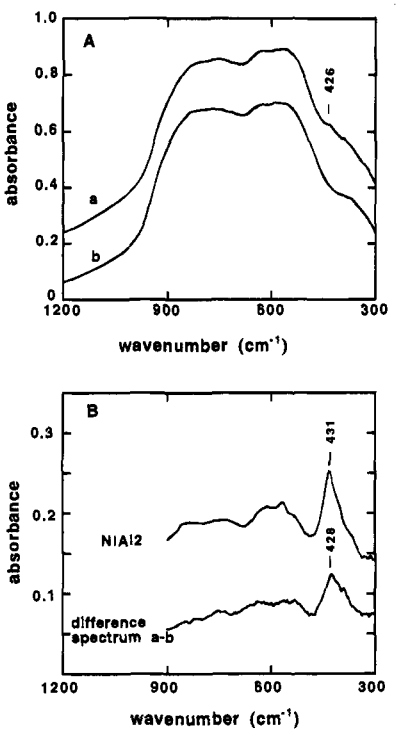

Figure 9. (A) IR spectra of the sample Ni4 (spectrum a) and of the blank Al_2O_3 impregnated at pH 7.2 without nickel and dried (spectrum b). (B) IR spectrum of an ill-crystallized NiAl2 reference compound and difference spectrum of the spectra presented in Figure 9A.

The spectrum of an ill-crystallized NiAl2 hydrotalcite is less resolved (Figure 9B). A broad band with ill-defined maxima appears in the 900−600 cm^{-1} range. Only the sharpest band around 430 cm^{-1} (although broadened) is still clearly visible.

In conclusion, the NiAl hydrotalcite compounds are characterized by a main vibration around 425−430 cm^{-1} which allows them to be distinguished clearly from hydroxides or basic nitrates. The position of this lattice vibration is independent of the crystalline state of hydrotalcite and is also observed in the CoAl hydrotalcites. IR spectroscopy is sensitive to the nature of the compensation anions. In particular, nitrates can be distinguished from carbonates as counterions.

(b) Characterization of the Ni/Al_2O_3 and Co/Al_2O_3 Samples. Figure 9A compares in the 1200−250 cm^{-1} frequency range the spectra of Ni4 sample (Table 3) and of the Al_2O_3 support conditioned at the same pH (7.2) as the Ni-containing sample (spectra a and b, respectively). These spectra show a broad band with maxima around 756 and 573 cm^{-1} corresponding to Al−O vibrations of the amorphous support. A shoulder in the 450−350 cm^{-1} range can be observed at a position close to hydrotalcite lattice vibrations in the spectrum of sample Ni4. In order to get more insight on the nature of the deposited phase, the difference of this spectrum and the spectrum of alumina was performed. This allowed minimization of the broad bands of the alumina support which partly inhibit the observation of hydrotalcite lattice bands. This method has already been employed with success to identify layered supported silicates of talc or serpentine structure, formed during the preparation of Ni/SiO_2 catalysts.[52] The difference spectrum shown in Figure 9B reveals the presence of a broad band at 428 cm^{-1}, which can be assigned to a poorly crystallized hydrotalcite-like compound (compare with the spectrum of a NiAl2 ill-crystallized hydrotalcite). The presence of significant amounts of nickel hydroxides or basic nitrates can be excluded. The weak and ill-defined peaks in the 900−500 cm^{-1} region correspond to the alumina support. The presence of hydrotalcite in sample Ni4 is therefore confirmed by IR spectroscopy. The counterions are nitrate ions which indicates that accumulation of carbonates during impregnation or storage in air is negligible. These results are valid for all the nickel-containing samples gathered in Table 3. The same results were obtained for the Co/Al_2O_3 samples. The formation of hydrotalcite-like phases in these samples is well accounted for by the presence of a band at 424 cm^{-1} (not shown here).

In conclusion, infrared spectroscopy is well adapted to identify Ni (Co) layered compounds on the basis of analysis of structural OH groups and lattice octahedral modes. IR also provides information on the nature of adsorbed or interlayer anions (carbonate or nitrate anions). The presence of hydrotalcite-like compounds was observed for the $Ni(Co)/Al_2O_3$ samples with nitrates as counterions.

Discussion

Currently, there are two traditional descriptions of the phenomena involved at the oxide/water interface in the presence of metal ions: the colloid and electrochemistry approach and the coordination chemistry approach. On the one hand, we are concerned with the electric double layer that forms at the oxide/liquid interface and by the question of location of the adsorbed metal ions. This approach has led to refined site binding models. On the other hand, we are concerned with the surface acting as a macroligand. Ion grafting is nothing more than a ligand exchange in the coordination sphere of the adsorbed ions. To a certain extent, the colloid chemistry approach highlights the point of view of oxide surfaces during impregnation whereas coordination chemistry highlights the point of view of the ion which interacts with a given adsorption site. Accordingly, it might seem that these approaches are complementary and should account for a comprehensive description of ion adsorption. This statement should be qualified:

(a) First, an ion which interacts with an OH^- or an O^{2-} does not identify it as belonging to the oxide, or to the hydrous oxide, or even to a supported hydroxide or coprecipitate. In other words, the coordination chemistry approach focuses on the local environment of adsorbed ions, with little consideration of effects beyond the nearest coordination sphere.

(b) Second, the chemical properties of oxide surfaces in the presence of water, metal ions, and ligands are certainly poorly represented by two-dimensional models directly issued from oxide/gas interfaces. Oxide rehydration as well as the formation of supported porous gels are phenomena which should not be overlooked. Likewise, while most of the site binding models are concerned with detailed descriptions of the electrolyte region at the oxide/solution interface, little is known about the effect of adsorbed ions on the support underneath the interface, in terms of charge polarization and weakening of the underlying bonds.

A realistic description of the oxide/water interfaces in the presence of metal ions and ligands should take into account effects of both sides of the oxide/liquid interface, i.e., the electrolyte *and* the support in the vicinity of the interface. In this paper, we examine a third approach, which uses geochemistry as a basis and which may fill the gap between the two existing approaches. The formation of coprecipitates under mild conditions, i.e., ambient temperature, pH close to the isoelectric point of the support, and reasonable contact times, shows that alumina can be reactive in the presence of metal ions and that not only the protons or OH^- ions are able to accelerate its dissolution.

(52) Kermarec, M.; Carriat, J.-Y.; Burratin, P.; Che, M.; Deccareau, A. *J. phys. Chem.* in press.

Growth of Hydrotalcite at a Distance from Alumina: Promotion of Alumina Dissolution by Ni(II) and Co(II) Ions. Let us now discuss the experiments leading to the formation of coprecipitates at a distance from alumina (using dialysis bags). These experiments were performed at pH and temperature conditions different from those used for the impregnations, namely pH 9 and 333 K. These modifications were dictated by the slow kinetics of the process, which is even slower at pH 7.2 and ambient temperature. Nevertheless, it is highly likely that the main conclusions reached in this section also apply to the latter pH and temperature conditions. A well-crystallized hydrotalcite-like phase is isolated outside the bag. The elemental analysis coupled with the lattice parameter determination by XRD indicate that there is probably no or very little amorphous phase in addition to hydrotalcite in the precipitate. In particular, the TG-DTA analysis, which is sensitive to composition heterogeneities in mixed precipitates or gels, confirms that there is no aluminum (oxy)hydroxide in addition to hydrotalcite.[31] The presence of hydrotalcite outside the bag implies that aluminum ions, possibly in combination with nickel ions, have come through the membrane. Since nickel ions are present outside and inside the bag, it is rather unlikely that aluminum ions are removed from the surface through the membrane to precipitate with nickel ions outside the bag. Hydrotalcite nuclei are most probably formed in the vicinity of the alumina surface, such as is the case during usual impregnations, then are free to move away from the alumina surface, under the effect of agitation, in particular through the membrane. The size of the nuclei has to be small enough to pass the membrane, i.e. around 10 nm. Finally the growth of these nuclei outside the membrane leads to well-crystallized hydrotalcite as shown in Figure 2. Thus, two results are noteworthy: first, aluminum can be extracted from the alumina surface under mild conditions to give rise to coprecipitates with Ni(II) ions; second, the coprecipitates formed during impregnation are not tightly bonded to the alumina surface.

The role of the Ni(II) or Co(II) ions (and possibly also of the nitrate ions) as promoters of the alumina dissolution at a pH close to its isoelectric point is highlighted. The nickel loading of sample Ni4 is 3.1 Ni wt % (Table 3). Hydrotalcite with a Ni/Al atomic ratio of about 1.4 is formed (Table 4), which corresponds to an aluminum content in the coprecipitate of around 1 wt % of the aluminum initially belonging to the support. Thus, 1 wt % of the alumina is dissolved after less than 1 h impregnation at pH 7.2! Likewise, the blank dialysis experiment performed at pH 9 and 333 K shows that the rate of alumina dissolution in these conditions is extremely low and it is even lower at ambient temperature and pH 7.2. This rate is, however, increased by three orders of magnitude by adding Ni(II) to the solutions, the other parameters including the ammonium nitrate concentration being kept constant. This clearly suggests that the breaking of Al−O bonds can be promoted not only by protons or OH^- ions but also by Ni(II) or Co(II) ions. It is likely that the Ni(II) or Co(II) ions have to adsorb onto the alumina surface before being able to promote the alumina dissolution. An important question is then, are adsorbed metal ions able to weaken underlying Al−O bonds at the alumina/water interface, for example, through polarizing the distribution of charges in some depth of the support? To our knowledge, only the influence of organic ligand-promoted dissolution has been investigated in detail.[4] Chelating agents can extract ions from otherwise insoluble oxides. For example, plants utilize chelating agents to extract ions from minerals and enable mineral weathering to take place at a much greater rate than would be indicated by simple inorganic considerations.[53] Inorganic ligands such as sulfite, phosphate, arsenate, chloride, and fluoride ions are also known to accelerate the dissolution of oxides in acid solutions.[54] Organic and inorganic dissolution-promoting and dissolution-inhibiting adsorbates have been reviewed for the Fe(III) oxides and hydroxides.[55] However, we are not aware of studies dealing with promotion or inhibition of oxide dissolution by adsorbed metal ions. Further investigation is clearly needed in this field.

XAS and IR Characterization of Hydrotalcite-Type Coprecipitates Including Al(III) Ions Extracted from the Support. Characterization techniques that can distinguish coprecipitates including aluminum ions from hydroxides or basic salts are important. Obviously, the greatest care has to be taken with the identification of hydrotalcite-like structures so as not to confuse them with precipitated hydroxides. The problem is not straightforward. The identification of coprecipitates by X-ray or electron diffraction is difficult. First, the supported phases are usually poorly crystallized. This is because they are formed at low temperatures without significant aging or ripening and also because oxide surfaces favor nucleation at the expense of particle growth. Second, more specifically, there is a strong analogy among the structures of the α-hydroxide, the basic salts, and the hydrotalcites. All are layer-type phases with interplanar distances ranging between 7 and 9 Å. Moreover, the cation−cation distances in the octahedral layers, i.e., the *a* parameter of the hexagonal cells, are only slightly different, see Table 1.

The XAS and IR spectroscopies are useful for obtaining more insight into the nature supported phases in wet or dried Ni/Al_2O_3 or Co/Al_2O_3 samples:

First, XANES spectroscopy as well as EXAFS analysis of the nearest coordination shell show that the deposited Ni and Co ions are octahedrally coordinated in the 2+ oxidation state independent of the metal loading and of the impregnation and drying parameters. In other words, the Ni and Co ions remain octahedrally coordinated in the 2+ state from the very beginning of impregnation until the drying step.

Second, infrared spectroscopy shows that nitrates are also adsorbed and are not removed by washing with distilled water. Thus, the adsorption of Co(II) or Ni(II) ions at near neutral pH leads in fact to the *coadsorption* of cations and anions. The substitution of nitrate by carbonate ions during impregnation or storage is negligible. Indeed, only traces of carbonates are detected by IR spectroscopy, and the thermogravimetric analysis coupled with mass spectrometry shows that only water and NOx are evolved upon heating. Thus, the precipitation of basic carbonates during impregnation or drying can be excluded.

Third, EXAFS analysis of the hydroxide, basic nitrate, and hydrotalcite-like reference compounds indicates that the EXAFS signals at the Ni or Co K edges are sensitive to the presence of aluminum in the octahedral layers, owing to the phase opposition between the Ni (or Co) and Al contributions in the hydrotalcite structure, see Figure 5. The presence of hydrotalcite in the samples gathered in Table 3 is readily demonstrated, see Figures 6 and 7 and Table 4. Furthermore, in these samples, the formation of hydrotalcite structure is quantitative, since EXAFS averages over all Ni- or Co-containing phases. Nevertheless, let us mention that the EXAFS technique is not sensitive to the nature of the counterions (nitrates or carbonates) required for electroneutrality of the hydrotalcites. An important point is that the XAS and IR determinations of hydrotalcite and hydroxide structures are unambiguous whatever the crystallinity of the

(53) Ollier, C. In *Geomorphology Texts: Weathering*; Clayton, K. M., Ed.; Longman: New York, 1983; pp 35−36.
(54) Grauer, R.; Stumm, W. *Colloid Polym. Sci.* **1982**, *260*, 959−970.
(55) Biber, M. V.; Dos Santos Afonso, M.; Stumm, W. *Geochim. Cosmochim. Acta* **1994**, *58*, 1999−2010.

structures may be. Poorly crystallized hydrotalcite-like structures cannot be confused with basic nitrates nor hydroxides. IR spectroscopy also enables one to distinguish hydrotalcite-like from basic nitrate and α-hydroxide structures. Infrared spectroscopy confirms the presence of aluminum in the precipitates through lattice vibrations characteristic of AlO_6 octahedra and provides additional information relative to the nature of the counterions present in the interlayers, namely nitrate ions for the Ni/Al_2O_3 and Co/Al_2O_3 samples and carbonate ions for the hydrotalcite-type reference compounds. The adsorption of anions is required for both electroneutrality and buildup of the deposited coprecipitates.

Toward a Unified Approach of the Phenomena Occurring at the Oxide/Water Interface in the Presence of Metal Ions Including Concepts from Geochemistry and Colloid and Coordination Chemistries. Concepts from colloid and coordination chemistries do not provide a comprehensive description of the phenomena occurring at the liquid/water interface in the presence of metal ions. Our knowledge of these interfaces can be greatly improved by concepts which use geochemistry as a basis, such as the formation of secondary minerals during natural or artificial weathering.

We suggest that three phenomena occur at the same time at the oxide/liquid interface: (1) the adsorption of ions, as described by electrostatic or site-binding models [the ions can be either electrostatically adsorbed (outer sphere complexes) or grafted (inner sphere complexes); in certain cases (as in this study) the adsorbed ions may even accelerate the rate of alumina dissolution]; (2) the dissolution of alumina, which is rate limiting [the dissolution rate is most probably dependent on the characteristics of the alumia surface, such as the area, the exposed faces (alumina structure), and the heterogeneities (impurities, defects)]; and (3) the precipitation of cations released from the support with metal ions in solution [this step is rapid and proceeds until the cation concentrations corresponding to the solubility products of the solid phases, i.e., alumina, hydrous alumina, and the coprecipitate (here, the hydrotalcite-like phase), are reached].

Alumina rehydration may also take place in addition to these phenomena. During the early stages of impregnation, ion adsorption occurs exclusively; then alumina passes slowly into solution and the first coprecipitate nuclei are quickly formed. The further steps consist of simultaneous ion adsorption and alumina dissolution. The aluminum ions which pass into solution precipitate quickly again with Ni(II) or Co(II) ions. The EXAFS characterization suggests that the amount of adsorbed ions is small during the coprecipitation process since the formation of hydrotalcite-like phases is quantitative in the analyzed samples. Finally, the result of this study is a rather complex description of the oxide/water interface, involving mass transfers from the solution to the solid and also from the solid to the solution.

Acknowledgment. We are very grateful to Mrs. C. Bobin for her help during analysis experiments. We express our thanks to Mrs. E. Leplat, B. Rebours, and the LURE staff for X-ray fluorescence measurements and for help during XRD and EXAFS measurements. Stimulating discussions with Dr. Ph. Courty, Dr. C. Marcilly, Prof. C. Bennett, and Prof. M. Che are also gratefully acknowledged.

Supporting Information Available: The Fourier transforms (k^3 weighing scheme; without phase correction) of the EXAFS of reference compounds shown in Figure 4, a statistical discussion of structural parameters derived from the EXAFS analysis, the XANES analysis of the Ni- and Co-containing samples and reference compounds (6 pages). This material is contained in many libraries on microfiche, immediately follows this article in the microfilm version of the journal, can be ordered from the ACS, and can be downloaded from the Internet; see any current masthead page for ordering information and Internet access instructions.

JA943846+